

Dark matter and Consequences of SUSY

Richard Arnowitt and Bhaskar Dutta[‡]

Center For Theoretical Physics, Department of Physics, Texas A&M University
College Station, TX 77843-4242, USA

Abstract. We examine here the constraints from the amount of relic density of neutralino dark matter and other experiments have on the SUSY parameter space for the mSUGRA model and for models with non-universal soft breaking at the GUT scale. In mSUGRA, the allowed amount of dark matter restricts the SUSY parameter space to a narrow band in $m_0 - m_{1/2}$ (except at very large $\tan\beta$). The Higgs mass and $b \rightarrow s\gamma$ constraints produce a lower bound of $m_{1/2} \gtrsim 300\text{GeV}$ and if the muon magnetic moment anomaly can be interpreted as a 3σ deviation from the Standard Model, one also obtains an upper bound of $m_{1/2} \lesssim 900\text{GeV}$, making the SUSY spectrum well accessible to the LHC. The $B_s \rightarrow \mu\mu$ decay is seen to be accessible to the Tevatron Run2B with 15fb^{-1} for $\tan\beta \gtrsim 30$. However, only parts of the spectrum will be accessible to the NLC if it's energy is below 800GeV . Non-universal soft breaking opens new regions of parameter space. Thus the $m_{1/2}$ lower bound constraint of $b \rightarrow s\gamma$ and also the Higgs mass can be reduced greatly if the gluino mass is assumed larger at the GUT scale (allowing for a lighter gaugino spectrum), and non-universal Higgs soft breaking masses at the GUT scale can open new allowed regions at relatively low $m_{1/2}$ and high m_0 where dark matter detection cross sections may be increased by a factor of ten or more.

1. Introduction

Supersymmetry is a natural solution to the gauge hierarchy problem that sets in for the Standard Model (SM) at the TeV scale. Thus if one supersymmetrizes the Standard Model particle spectra, one can build a model going past the TeV scale yet consistent with all the successes of the Standard Model below 1 TeV. If one continues such models to yet higher energies, one find the remarkable grand unification of the three gauge coupling constants at the GUT scale $M_G \cong 2 \times 10^{16}\text{ GeV}$, a result consistent with the LEP data at the percent level. Theoretical models which yield this unification arise naturally in supergravity (SUGRA) grand unification[1, 2], and such models with R-parity invariance have the additional remarkable feature of predicting the existence of cold dark matter (CDM)[3, 4], the lightest neutralino $\tilde{\chi}_1^0$, with a relic density amount comparable to what is observed.

We discuss here some of the other consequences that might be expected of such SUGRA models. Already existing experiments have begun to restrict the SUSY parameter space significantly. Most significant of these are the amount of CDM, the Higgs mass bound, the $b \rightarrow s\gamma$ branching ratio, and (possibly) the muon a_μ anomaly. We start the discussion

[‡] Present Address: Department of Physics, University of Regina, Regina SK, S4S 0A2 Canada

with the simplest model, mSUGRA, with universal soft breaking parameters, and discuss additional signatures of SUSY that might be seen at accelerators, i.e. the $B_s \rightarrow \mu^+ + \mu^-$ decay at the Tevatron, and the processes $e^+ + e^- \rightarrow \tilde{\tau}_1^+ + \tilde{\tau}_1^-$ or $e^+ + e^- \rightarrow \tilde{\chi}_1^0 + \tilde{\chi}_2^0$ at future linear colliders (LC). We will then consider non-universal models (with non-universal gaugino masses and non universal Higgs soft breaking masses at M_G) to see how robust the mSUGRA predictions are, and where non-universal soft breaking signals might reside.

2. mSUGRA Models

The mSUGRA models[1, 2] depend on four extra parameters and one sign (and as such is the most predictive of the SUSY models). We take these to be m_0 (the universal scalar soft breaking mass at M_G), $m_{1/2}$ (the universal gaugino masses at M_G), A_0 (the cubic soft breaking mass at M_G), $\tan \beta = \langle H_2 \rangle / \langle H_1 \rangle$ (at the electroweak scale), and the sign of the Higgs mixing parameter μ (which appears in the superpotential W as $\mu H_1 H_2$). We examine the parameter range $m_0 > 0$, $m_{1/2} \leq 1$ TeV (which corresponds to the LHC reach of $m_{\tilde{g}} < 2.5$ TeV), $2 < \tan \beta < 55$ and $|A_0| < 4m_{1/2}$.

mSUGRA makes predictions about two items involving dark matter: the neutralino-nucleus cross section being looked for by terrestrial detectors of dark matter from the Milky Way halo, and the mean amount of relic dark matter in the universe left over from the Big Bang. For detectors with heavy nuclei in their targets, the spin independent $\tilde{\chi}_1^0$ -nucleus cross section dominates, which allows one to extract the $\tilde{\chi}_1^0$ -proton cross section $\sigma_{\tilde{\chi}_1^0-p}$. The basic quark diagrams here are the scattering through s-channel squarks, and t-channel CP even Higgs bosons, h and H . For the relic density analysis, one must calculate the neutralino annihilation cross section in the early universe which proceeds through s channel Z and Higgs poles (h , H , A) and t-channel sfermions. However, if a second particle becomes nearly degenerate with the $\tilde{\chi}_1^0$, one must include it in the annihilation channels which leads to the phenomena of co-annihilation. In SUGRA models, this accidental near degeneracy occurs naturally for the light stau, $\tilde{\tau}_1$. One can see this qualitatively for low and intermediate $\tan \beta$ where one can solve the RGE analytically. Thus for the right selectron, e_R , one finds

$$m_{e_R}^2 = m_0^2 + 0.15m_{1/2}^2 - \sin^2\theta_W M_W^2 \cos 2\beta, \quad (1)$$

$$M_{\tilde{\chi}_1^0}^2 = 0.16m_{1/2}^2 \quad (2)$$

For $m_0 = 0$, the two become degenerate at $m_{1/2} \cong 350$ GeV, and co-annihilation thus begins at $m_{1/2} \cong 350$ GeV (more precisely for the $\tilde{\tau}_1$ which is the lightest slepton). As $m_{1/2}$ increases, m_0 must increase (to keep the $\tilde{\tau}_1$ heavier than the $\tilde{\chi}_1^0$) and one gets narrow bands of allowed regions in the $m_0 - m_{1/2}$ plane for each $\tan \beta$ and A_0 .

One starts the analysis at the M_G and uses the renormalization group equations (RGE) to obtain predictions at the electroweak scale. In carrying out these calculation, it is necessary to include a number of corrections and we list some of these here: (1) We use two loop gauge and one loop Yukawa RGE in running from M_G to the electroweak scale M_{EW} , and three loop QCD RGE below M_{EW} for light quark contributions. (2) Two loop and pole mass corrections are included in the calculation of m_h . (3) One loop correction to m_b and m_τ are included[5]

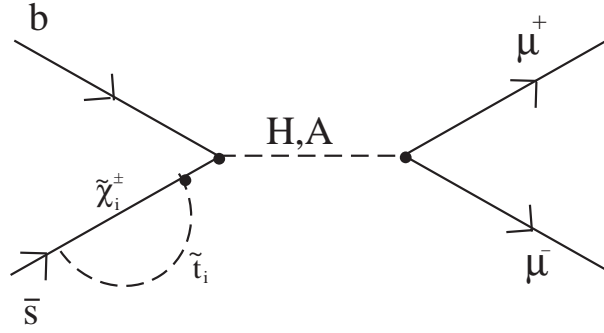


Figure 1. Example of a leading contribution to the decay $B_s \rightarrow \mu\mu$. Each vertex with a dot has a factor of $\tan\beta$ so that the diagram is proportional to $\tan^3\beta$.

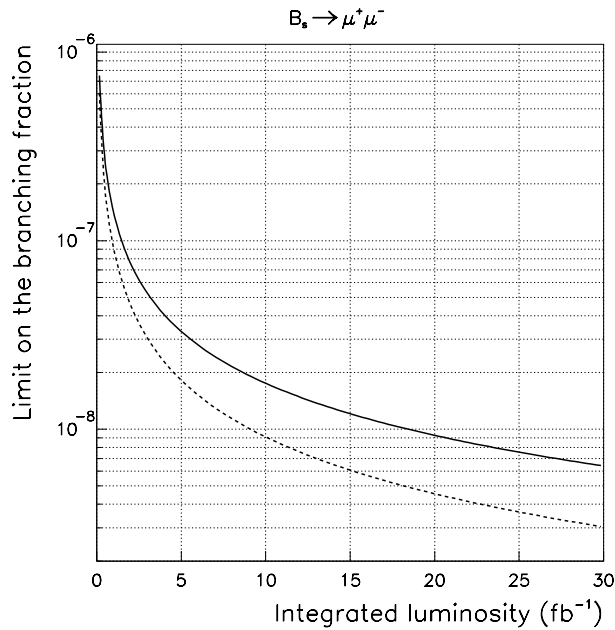


Figure 2. Expected sensitivity to $B_s \rightarrow \mu\mu$ of the CDF detector as a function of luminosity. The solid curve is a conservative estimate, and the dotted curve gives a limiting sensitivity.[20]

(4) All stau-neutralino co-annihilation channels are included in the relic density calculation [6, 7, 8]. (Chargino-neutralino co-annihilation does not occur for $m_{1/2} < 1$ TeV.) Large $\tan\beta$ NLO SUSY corrections to $b \rightarrow s\gamma$ are included[9, 10, 11]. We do not include Yukawa unifications or proton decay constraints as these depend sensitively on post-GUT physics, about which little is known.

We use the following experimental input to constrain the SUSY parameter space: (1) Global fits for the CMB and other astronomical measurements now restrict the amount of CDM considerably[12]. We use here the range:

$$0.07 < \Omega_{\text{CDM}} h^2 < 0.21 \quad (3)$$

The MAP data, due out perhaps early next year should be able to restrict this range considerably.

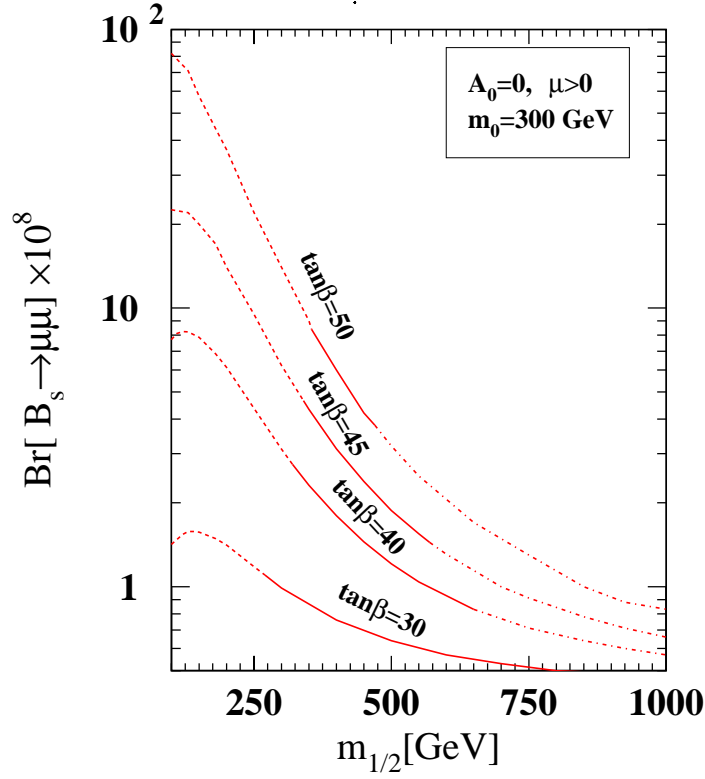


Figure 3. mSUGRA predicted values of $B(B_s \rightarrow \mu\mu)$ for different values of $\tan\beta$ for $A_0 = 0$ and $m_0 = 300$.

(2) The LEP lower bound $m_h > 114$ GeV[13], is a significant constraint for $\tan\beta \lesssim 30$, and in fact an increase of three to five GeV would cover most of the parameter space. Unfortunately, however, the theoretical evaluation of m_h still has an error of $\sim (2 - 3)$ GeV, and so we interpret the LEP bound to mean $(m_h)^{theory} > 111$ GeV.

(3) The CLEO data for the decay $b \rightarrow s\gamma$ [14] has both systematic and theoretical error, and so we use a relatively broad range for the branching ratio around the CLEO central data:

$$1.8 \times 10^{-4} < B(B \rightarrow X_s\gamma) < 4.5 \times 10^{-4} \quad (4)$$

The $b \rightarrow s\gamma$ rate produces a significant constraint for large $\tan\beta$.

(4) Shortly after this conference, the Brookhaven E821 experiment published new results of their measurement of the muon anomaly[15] which reduced the statistical error by a factor of 2 (and the systematic error somewhat). Also new more accurate data from CMD-2, BES, ALEPH and CLEO have allowed a more accurate determination of the SM contribution to a_μ , and there have been two new evaluations of this [16, 17] (See also talk by T. Teubner at this conference). If the $e^+ - e^-$ data is used to calculate the SM contribution, both groups find a 3σ deviation between experiment and the SM prediction e.g.[16]

$$\Delta a_\mu = 33.9(11.2) \times 10^{-10} \quad (5)$$

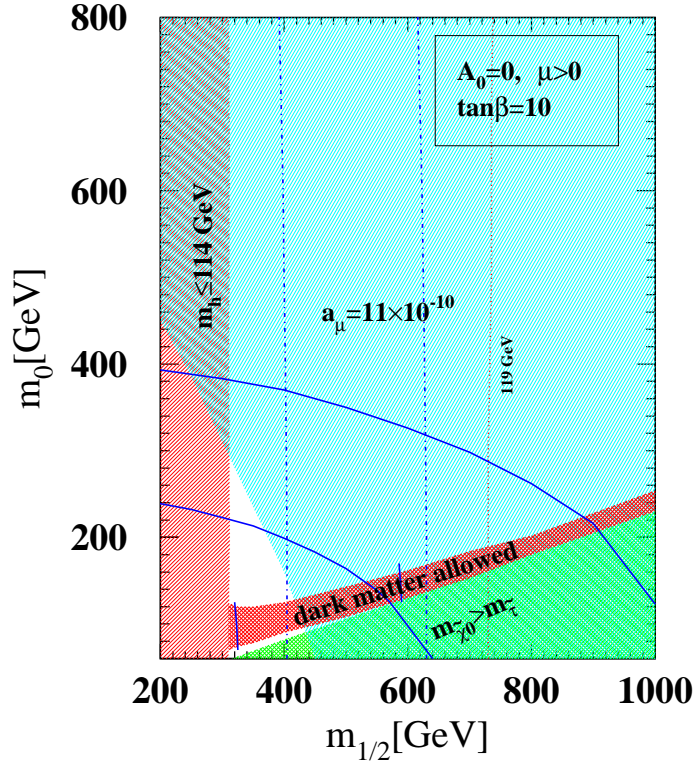


Figure 4. mSUGRA allowed region for $\tan \beta = 10$, $A_0 = 0$, $\mu > 0$. The shaded upper right region is forbidden by the a_μ bound at the 2σ level if Eq. (5) is valid. The dot-dash lines are for the LC $\tilde{\chi}_1^0 - \tilde{\chi}_2^0$ signal for the 500GeV machine (left line) and 800GeV machine (right line). (The LC is sensitive to regions to left of the line.) The curved solid lines are for the LC $\tilde{\tau}_1 - \tilde{\tau}_1$ signal (the lower one for the 500 GeV machine and the higher one for the 800GeV machine). The short vertical lines are for DM detection cross sections, $\sigma_{\tilde{\chi}_1^0 - p} = 5 \times 10^{-9}$ pb (left line) and 1×10^{-9} pb (right).

On the other hand if the tau data of ALEPH and CLEO are used (with appropriate CVC breakdown corrections) the deviation from the SM is reduced to only 1.6σ and the two evaluations are statistically inconsistent [16]. The matter remains unclear as to which result is correct. In order to see the significance of Eq. (5), we will here use this result, and assume a 2σ lower bound on Δa_μ exists and that this is attributable to SUSY. SUSY, in fact makes a significant contribution to a_μ , and if a_μ^{SUSY} were $\lesssim 10^{-10}$, the squark and gluino mass spectrum would be pushed into the TeV domain.

The combination of the m_h (for low $\tan \beta$) and $b \rightarrow s\gamma$ (for high $\tan \beta$) constraints produces a lower bound on $m_{1/2}$ over the entire parameter space of $m_{1/2} \gtrsim (300-400)\text{GeV}$, and consequently $m_{\tilde{\chi}_1^0} \gtrsim (120 - 160)\text{GeV}$. This means that most of the parameter space is in the $\tilde{\tau}_1 - \tilde{\chi}_1^0$ co-annihilation domain, and hence in order to satisfy the CDM amount, m_0 is approximately determined by $m_{1/2}$ (for fixed $\tan \beta$, A_0). The sign of μ and Δa_μ are correlated [18, 19], and so the assumption of Eq. (5) means that $\mu > 0$.

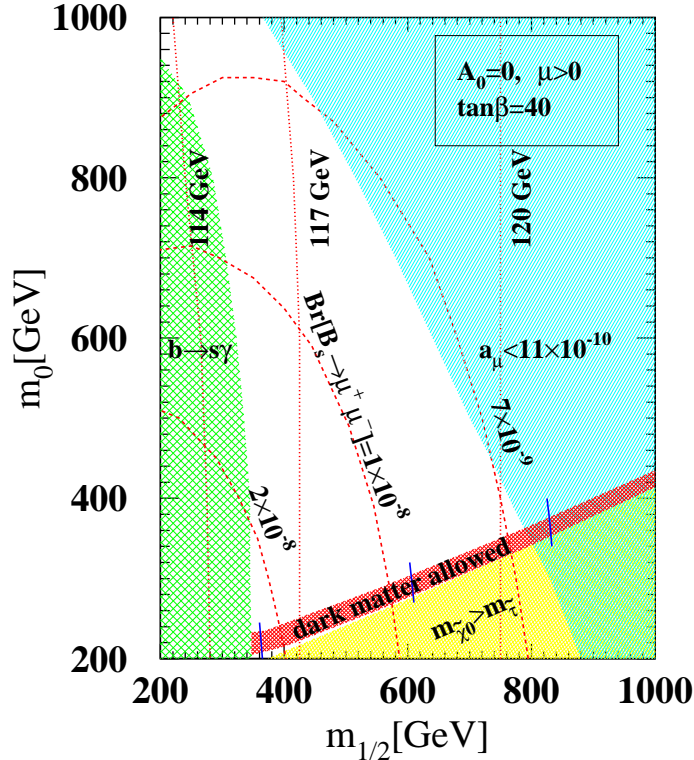


Figure 5. The same as Fig. 4 for $\tan\beta = 40$, $A_0 = 0$, the dashed lines giving contours of $B_s \rightarrow \mu\mu$ branching ratios. The lower short vertical line is $\sigma_{\tilde{\chi}_1^0-p} = 3 \times 10^{-8}$ pb and the upper one is 1×10^{-9} pb

3. SUSY Signals At The Tevatron and Linear Colliders

Before examining in more detail the effects of existing experiments on the SUSY parameter space, we discuss the $B_s \rightarrow \mu\mu$ decay at the Tevatron and also examine SUSY signals that might survive at a linear collider.

The $B_s \rightarrow \mu\mu$ opens an additional window at the Tevatron for investigating the mSUGRA parameter space [20, 21, 22, 23]. The SM predicts a very small branching ratio of $B[B_s \rightarrow \mu\mu] = (3.1 \pm 1.4) \times 10^{-9}$. Further, the SUSY contribution can become quite large for large $\tan\beta$, as the leading diagrams (an example is given in Fig. 1) grow like $\tan\beta^3$ and hence the branching ratio grows as $\tan\beta^6$. A set of cuts have been obtained eliminating background (mostly gluon splitting $g \rightarrow b\bar{b}$ and fakes) [21] leading to a sensitivity of $B[B_s \rightarrow \mu\mu] \gtrsim 6 \times 10^{-9}$ for 15fb^{-1} /detector. Fig. 2 shows the sensitivity (for a single detector) as a function of luminosity, and Fig. 3 shows the expected mSUGRA branching ratio for different $\tan\beta$ for the example of $A_0 = 0$, $m_0 = 300\text{GeV}$. One sees that the Tevatron will be sensitive to this decay for $\tan\beta \gtrsim 30$.

It is interesting to examine what possible SUSY signals of mSUGRA a linear collider might see. We consider here two possibilities: $\sqrt{s} = 500\text{GeV}$ and $\sqrt{s} = 800\text{GeV}$. We've seen above that the m_h and $b \rightarrow s\gamma$ constraint already mean that $m_{1/2} > (350 - 400)\text{GeV}$, and

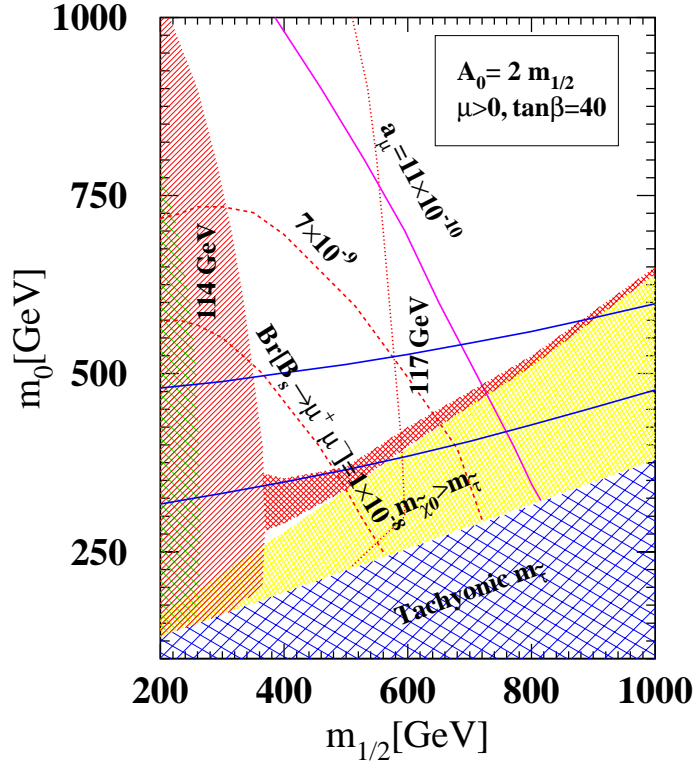


Figure 6. Same as Fig. 5 for $\tan \beta = 40$, $A_0 = 2m_{1/2}$, $\mu > 0$.

so for mSUGRA this means that gluinos and squarks would generally be beyond the reach of such machines (as well as selectrons and smuons for a large part of the parameter space). The most favorable SUSY signals are then

$$\begin{aligned} e^+ + e^- &\rightarrow \tilde{\chi}_2^0 + \tilde{\chi}_1^0 \rightarrow (l^+ + l^- + \tilde{\chi}_1^0) + \tilde{\chi}_1^0 \\ e^+ + e^- &\rightarrow \tilde{\tau}_1^+ + \tilde{\tau}_1^- \rightarrow (\tau + \tilde{\chi}_1^0) + (\tau + \tilde{\chi}_1^0) \end{aligned} \quad (6)$$

where l^+ or l^- means any charged lepton. Since for mSUGRA one has that $m_{\tilde{\chi}_2^0} \simeq 2m_{\tilde{\chi}_1^0}$, the mass reach for these particle are

$$1/2m_{\tilde{\chi}_2^0} \simeq m_{\tilde{\chi}_1^0} \lesssim 165(265) \quad (7)$$

$$m_{\tilde{\tau}_1} \lesssim 250(400) \text{ GeV for } \sqrt{s} = 500(800) \quad (8)$$

There are a number of SM backgrounds that have to be considered to see if a clean signal remains. For example, WW production with decay into tau final states can be controlled by polarizing the beams. Cuts to eliminate other possible backgrounds are under consideration[24].

4. The mSUGRA Parameter Space

We now summarize the effects of the constraints from m_h , $b \rightarrow s\gamma$, dark matter density and a_μ on the mSUGRA parameter space, and also what might be expected from the $B_s \rightarrow \mu\mu$

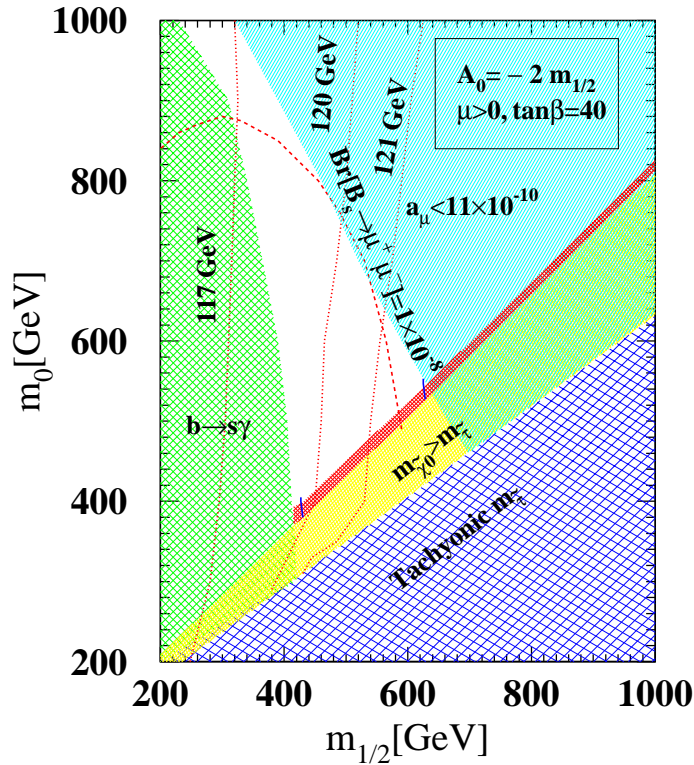


Figure 7. Same as Fig. 5 for $\tan\beta = 40$, $A_0 = -2m_{1/2}$, $\mu > 0$

observation at the Tevatron and linear collider (LC) signals. Fig. 4 exhibits the parameter space for $\tan\beta = 10$, $A_0 = 0$. One sees that the a_μ bound (if valid) combined with the m_h bound and the relic density constraint leaves very little parameter space at low $\tan\beta$. Either of the two linear collider signals could scan the full remaining space. The dark matter detection cross sections are of size that would be observable by the planned future DM detectors. Figs. 5,6,7 for $\tan\beta = 40$, $A_0 = 0$, $2m_{1/2}$ and $-2m_{1/2}$ exhibit a larger allowed parameter space. The Tevatron's $B_s \rightarrow \mu\mu$ covers the full allowed region for $A_0 = 0$ and $-2m_{1/2}$, and about half the space for $A_0 = 2m_{1/2}$. In each case, the NLC at 500GeV can only cover a part of the parameter space. We note that the stau-stau LC signal extends to high $m_{1/2}$ and relatively low m_0 , while the $\tilde{\chi}_1^0 - \tilde{\chi}_2^0$ signal can cover large m_0 but limited $m_{1/2}$. In view of the nature of the allowed DM channel, the former is of more significance. At very high $\tan\beta$, a bulge in the DM allowed channel develops at low $m_{1/2}$ due to the fact the heavy Higgs (A, H) become light, allowing a rapid early universe annihilation through the A and H s-channel diagrams. This is shown most dramatically in Fig. 8 for $\tan\beta = 55$, $A_0 = 0$. Here even the 800 GeV LC cannot cover the full parameter space, though the Tevatron signal of $B_s \rightarrow \mu\mu$ would be observable over the full parameter space.

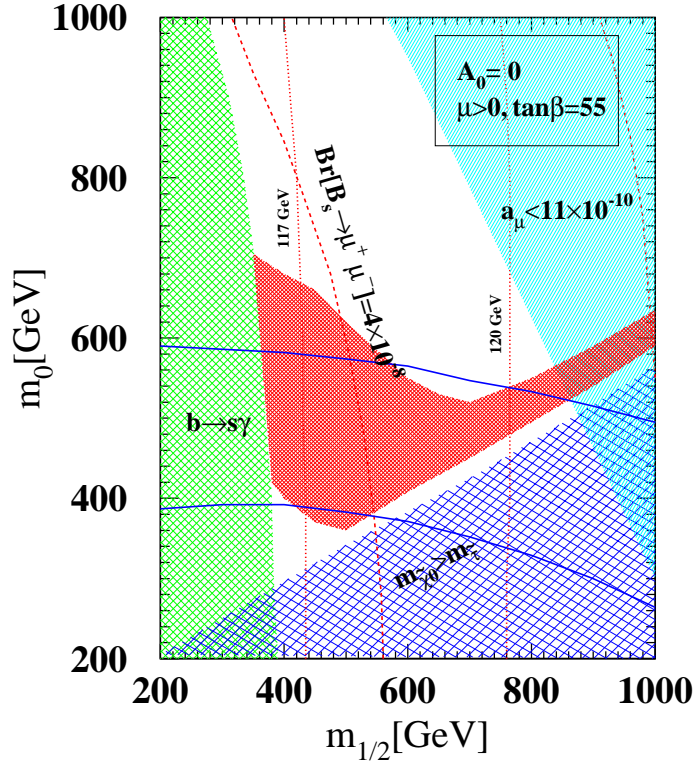


Figure 8. Same as Fig. 5 for $\tan\beta = 55$, $A_0 = 0$, $\mu > 0$ and $m_t = 175\text{GeV}$, $m_b = 4.25$. (Note that the results are sensitive to the exact values of m_t and m_b used)

5. Non-Universal Models

We examine next some SUGRA models with non-universal soft breaking to see what aspects of the results of Sec. 4 are maintained. We consider specifically the case of non-universal gaugino masses and non-universal Higgs soft breaking masses at M_G . Two striking effects in mSUGRA are the $\tilde{\chi}_1^0 - \tilde{\tau}_1$ co-annihilation channel which leads to a narrow band in the $m_{1/2} - m_0$ plane of allowed relic density, and the fact that the combined effects of $b \rightarrow s\gamma$ and the m_h bounds require $m_{\tilde{\chi}_1^0} \gtrsim 120$ (i.e. $m_{1/2} \gtrsim 300\text{GeV}$).

The possibility of non-universal gaugino masses at M_G can relax significantly the constraints of $b \rightarrow s\gamma$ and m_h . Thus if the gluino mass is increased, it effects the stop mass which has major effects on both $b \rightarrow s\gamma$ and m_h . For example, a gluino mass which is twice the universal value at M_G reduces the lower bound on $m_{\tilde{\chi}_1^0}$ to 75GeV ($m_{1/2} \gtrsim 190\text{GeV}$) and also $m_{\tilde{\chi}_1^\pm}$ to $\sim 150\text{GeV}$, making these particles more accessible. On the other hand, the near degeneracy between $\tilde{\tau}_1$ and $\tilde{\chi}_1^0$ remains, since this depends mainly on the U(1) gaugino mass \tilde{m}_1 . Non-universality in the Higgs masses at M_G , i. e. $m_{H_{1,2}}^2 = m_0^2(1 + \delta_{1,2})$, can also produce new effects. While this introduces two additional parameters into the model, one can understand their effects since μ^2 controls much of the physics. Thus if μ^2 decreases, the Higgsino content of the neutralino increases and this has two effects: it increases the

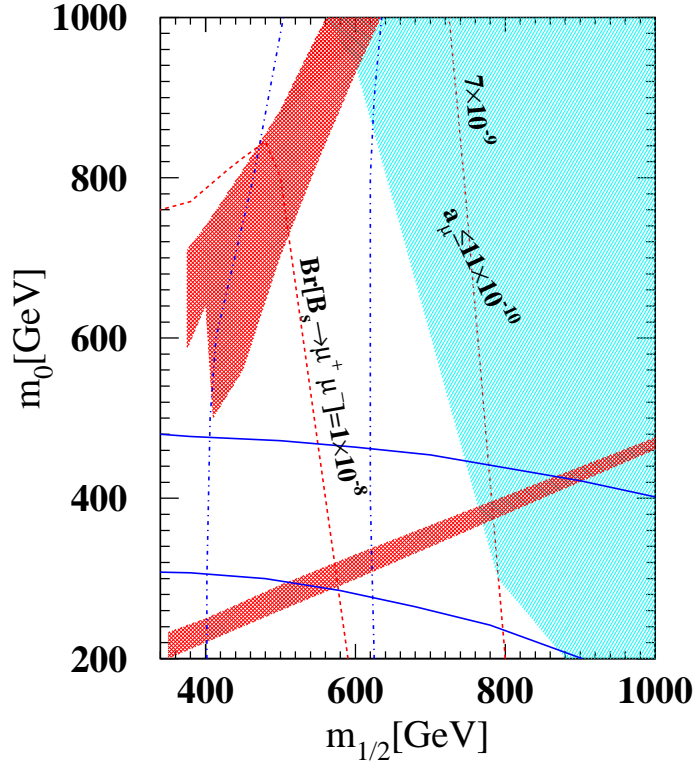


Figure 9. Same as Fig. 5 for $\delta_2 = 1$, $\tan \beta = 40$, $A_0 = m_{1/2}$, $\mu > 0$. The shaded region for large m_0 and low $m_{1/2}$ is due to the increased annihilation through the Z-channel. The lower stau-neutralino narrow band is essentially unchanged.

$\tilde{\chi}_1^0 - \tilde{\chi}_1^0 - Z$ coupling and also $\sigma_{\tilde{\chi}_1^0 - p}$. To see what effects occur qualitatively, we note that for small and intermediate $\tan \beta$ the RGE can be solved analytically and give

$$\mu^2 = (\mu^2)_{\text{mSUGRA}} + t^2/(t^2 - 1)[-1/2(1 + D_0)\delta_2 + \delta_1/t^2]m_0^2 \quad (9)$$

where $t = \tan \beta$, $D_0 \cong 1 - (m_t/200 \sin \beta)^2 \cong 0.25$. A positive δ_2 then decreases μ^2 while μ^2 is relatively insensitive to δ_1 . Fig. 9 exhibits the allowed relic density regions for the case of $\delta_2 = 1$, $\tan \beta = 40$, $A_0 = m_{1/2}$. One sees that a new region of allowed relic density arises for small $m_{1/2}$ and large m_0 from the increased annihilation through the Z s-channel. (The usual $\tilde{\tau}_1 - \tilde{\chi}_1^0$ co-annihilation region is present also.) This region is mostly unobservable at a 500GeV NLC. Fig. 10 shows the corresponding DM cross sections. The Z-channel region can increase $\sigma_{\tilde{\chi}_1^0 - p}$ by a factor of 10 or more.

6. Conclusions and Summary

We have discussed here the current restrictions on the SUSY parameter space from existing experiments and what may be obtained from future experiments at the Tevatron (from the $B_s \rightarrow \mu\mu$ decay) and from linear colliders (using $\tilde{\tau}_1 - \tilde{\tau}_1$ and $\tilde{\chi}_1^0 - \tilde{\chi}_2^0$ signals). We have examined mSUGRA models and also non-universal SUGRA models.

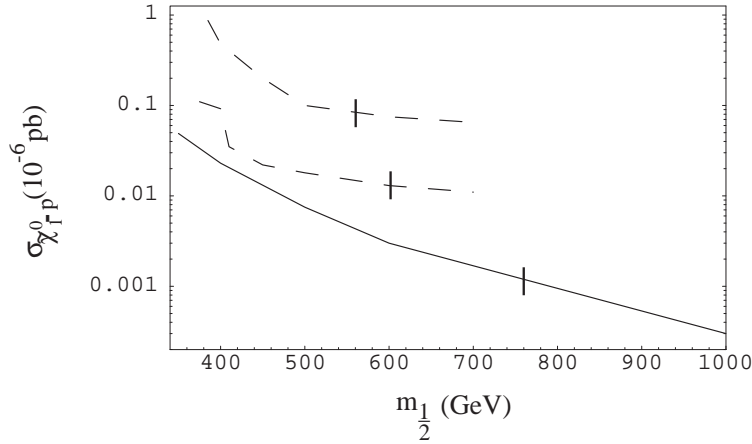


Figure 10. Dark matter detection cross section for $\tan\beta = 40$, $A_0 = m_{1/2}$, $\mu > 0$, $\delta_2 = 1$. The upper dashed band is the new region due to the increased Z-channel annihilation. The lower line is the upper value from the narrow $\tilde{\tau}_1 - \tilde{\chi}_1^0$ co-annihilation channel. The short vertical lines are the 2σ bound from the a_μ anomaly.

For mSUGRA one finds the $\tilde{\tau}_1 - \tilde{\chi}_1^0$ co-annihilation limits the allowed parameter space to a narrow band except for large $\tan\beta$. The combined $b \rightarrow s\gamma$ and m_h bounds then requires $m_{\tilde{\chi}_1^0} \gtrsim 120\text{GeV}$, forbidding a light neutralino. The Tevatron with 15fb^{-1} /detector luminosity could scan almost the entire parameter space for $\tan\beta \gtrsim 40$ (if $a_\mu^{\text{SUSY}} \gtrsim 10 \times 10^{10}$) using the $B_s \rightarrow \mu\mu$ decay. A linear collider at 800GeV can scan almost all the parameter space, though a 500GeV machine would miss much of the parameter space for large $\tan\beta$. Dark matter detection cross sections are all within the range of sensitivity for planned detectors (i.e. $\gtrsim 10^{-10}\text{pb}$).

Non-universal models introduce new phenomena. Thus a non-universal gluino mass can greatly weaken the lower bound on $m_{\tilde{\chi}_1^0}$ due to $b \rightarrow s\gamma$ and m_h . An increased non-universal H_2 Higgs mass at M_G can give rise to a new region of allowed relic density for low $m_{1/2}$ and large m_0 from rapid Z-channel annihilation, while maintaining the usual $\tilde{\tau}_1 - \tilde{\chi}_1^0$ co-annihilation channel. The dark matter cross sections can increase by a factor of 10 or more in the new Z-channel region.

Acknowledgement

This work was supported in part by the National Science Foundation Grant PHY - 0101015.

References

- [1] A.H. Chamseddine, R. Arnowitt, P. Nath, Phys. Rev. Lett. 49 (1982) 970.
- [2] L. Hall, J. Lykken, S. Weinberg, Phys. Rev. D27 (1983) 2359; P. Nath, R. Arnowitt, A.H. Chamseddine, Nucl. Phys. B227 (1983) 12.
- [3] H. Goldberg, Phys. Rev. Lett.50(1983)1419.
- [4] J. Ellis, J. Hagelin, D. Nanopoulos, K. Olive, M. Srednicki, Nucl. Phys. B 238(1984)453.

-
- [5] R. Rattazi, U. Sarid, *Phys. Rev. D* 53(1996)1553; M. Carena, M. Olechowski, S. Pokorski, C. Wagner, *Nucl. Phys. B* 426(1994)269.
- [6] R. Arnowitt, B. Dutta, Y. Santoso 2000 [hep-ph/0010244](#); 2001 [hep-ph/0101020](#); *Nucl. Phys. B* 606(2001)59.
- [7] J. Ellis, T. Falk, G. Gani, K. Olive, M. Srednicki 2001 *Phys. Lett. B* 570(2001)236; J. Ellis, T. Falk, K. Olive, *Phys. Lett. B* 444 (1998)367; J. Ellis, T. Falk, K. Olive, M. Srednicki, *Astropart. Phys.* 13(2000)181; Erratum-ibid. 15(2001)413.
- [8] M. Gomez, J. Vergados [hep-ph/0012020](#); M. Gomez, G. Lazarides, C. Pallis, *Phys. Rev. D* 61 (2000)123512; *Phys. Lett. B* 487(2000)313; L. Roszkowski, R. Austri, T. Nihei, *JHEP* 0108(2001)024; A. Lahanas, D. Nanopoulos, V. Spanos, *Phys. Lett. B* 518(2001)518.
- [9] G. Degrassi, P. Gambino, G. Giudice 2000 *JHEP* 0012(2000)009.
- [10] M. Carena, D. Garcia, U. Nierste, C. Wagner 2001 *Phys. Lett. B* 499(2001)141.
- [11] D'Ambrosio, Giudice, Isidori, Strumia, [hep-ph/0207036](#); A. Buras, P. Chankowski, J. Rosiek and L. Slawianowska, [hep-ph/0210145](#).
- [12] M. Turner 2002, [astro-ph/0202007](#).
- [13] P. Igo-Kemenes, LEP meeting, 2000 (<http://lephiggs.web.cern.ch/LEPHIGGS/talks/index.html>).
- [14] M. Alam et al, *Phys. Rev. Lett.* 74(1995)2885.
- [15] G. Bennett et al., Muon (g-2) Collaboration, 2002 *Phys. Rev. Lett.* 89 101804.
- [16] M. Davier, S. Eidelman, A. Hocker, Z. Zhang, 2002 [hep-ph/0208177](#).
- [17] K. Hagiwara, A. Martin, D. Nomura, T. Teubner, 2002 [hep-ph/0209187](#).
- [18] J.L. Lopez, D.V. Nanopoulos, X. Wang, *Phys. Rev. D* 49(1994)366.
- [19] U. Chattopadhyay, Pran Nath 1996 *Phys. Rev. D* 531648.
- [20] C. Bobeth, T. Ewerth, F. Kruger, J. Urban 2001 *Phys. Rev. D* 64(2001)074014.
- [21] R. Arnowitt, B. Dutta, T. Kamon, M. Tanaka, *Phys. Lett. B* 538(2002)121.
- [22] A. Dedes, H.K. Dreiner, U. Nierste, *Phys. Rev. Lett.* 87(2001)251804.
- [23] S. Mizukoshi, X. Tata, Y. Wang, [hep-ph/0208078](#).
- [24] R. Arnowitt, B. Dutta, T. Kamon, V. Khotilovich, work in progress